Enhanced Ordering of Liquid Crystalline Suspensions of Cellulose Microfibrils: A Small Angle Neutron Scattering Study

W. J. Orts*

U.S. Department of Agriculture, Western Regional Research Center, 800 Buchanan Street, Albany, California 94710

L. Godbout and R. H. Marchessault

PAPRICAN and Chemistry Department, Pulp and Paper Research Centre, McGill University, 3420 University Street, Montreal, PQ, Canada H3A 2A7

J.-F. Revol

PAPRICAN, 570 boul St-Jean, Pointe-Claire, PQ, Canada H9R 3J9

Received July 29, 1997; Revised Manuscript Received June 1, 1998

ABSTRACT: Small angle neutron scattering, SANS, was used to characterize the enhanced ordering induced by magnetic and shear alignment of chiral nematic liquid crystals of cellulose microfibrils in aqueous suspension. In a ∼2 T magnetic field the chiral nematic phase exhibits a uniform orientation over an entire 10 mL sample. SANS data confirmed that the cholesteric axis of this phase aligns along the magnetic field with implications that the distance between microfibrils is shorter along the cholesteric axis than perpendicular to it. This is consistent with the hypothesis that cellulose microfibrils are helically twisted rods. Under shear flow, the alignment of microfibrils changes from chiral nematic to nematic with relative order increasing with increasing shear rate. The axial ratio (length/width) is the key parameter in determining the relative order achieved and in determining the relaxation behavior after shear ceases.

Introduction

The reaction of cellulose with sulfuric, phosphoric, or other mineral acids is well-known for making cellulose esters. Although reaction conditions can lead to dissolution, derivitization, or hydrolysis, there are specific windows where the stringlike cellulose fibrils hydrolyze randomly to form colloidal rods. These microfibrillar fragments are crystallites with nearly single-crystal perfection. A few sulfate or phosphate ester groups at the crystallite surfaces provide anionic stabilization via the attraction/repulsion forces of electrical double layers.[1]

The electron microscope permitted researchers such as Ranby and colleagues[2] to identify that acid-hydrolyzed native cellulose fibers in water are colloidal suspensions of individual crystallites. After hydrolysis conditions were optimized,[3] Marchessault et al.[1] showed that cellulose colloidal suspensions exhibit nematic liquid crystalline alignment. Nematic ordering is the alignment of fibrils in the same direction along a *director* and has long been sought after in the fiber industry with the promise of higher tensile strengths.

In a more recent discovery, Revol et al.[4−7] formed suspensions of acid hydrolyzed cellulose microfibrils exhibiting chiral nematic (cholesteric) ordering. Chiral nematic ordering is often described in simple terms as the helicoidal stacking of *nematic planes*. As shown in Figure 1a, rods within a plane are aligned along a director, and these nematic planes are stacked such that the angle of the director in each subsequent plane is offset incrementally. This results in a "spiral staircase" packing of microfibrils around a *cholesteric axis*. For acid-hydrolyzed suspensions of cellulose microfibrils,[4] the chiral nematic phase forms at critical concentrations greater than ∼1.5% (w/w), a low concentration relative to the onset of liquid crystalline behavior for other polymer materials. This is most likely because the crystallites are stiff over their entire length, with persistence lengths approaching their axial dimension.[4] Formation of the chiral nematic phase is highlighted by the presence of tactoids—domains of uniform order ranging in size from 20 to 150 μm. Disruption of these domains will certainly affect the shear behavior of these suspensions. Interestingly, magnetic fields (>1 T) also break down these domains to form a single phase of chiral nematic ordering with the cholesteric axis aligned parallel to the field direction.[5]

Liquid crystalline suspensions of cellulose microfibrils are particularly attractive because of their simplicity; consisting of charged microfibrils that "self-assemble" into large regions of cholesteric ordering. Until this discovery, it was assumed that the helicoidal arrangement of cellulose microfibrils found in the structural systems of plants was due to an additional asymmetric "twisting agent", which induces cholesteric packing. Since no obvious asymmetric molecules are present in these model suspensions (or in chitin suspensions that exhibit similar ordering), Revol and Marchessault[6] hypothesized that there must be a twist in the microfibrils themselves that accounts for their chiral interaction.

Revol et al.[7] have taken advantage of this cholesteric ordering to form cellulosic films with unique and controllable optical properties. The cholesteric pitch (or distance between nematic planes) of the cellulose microfibrils in the dried films is in the same length scale as the wavelength of visible light. This creates an interference device that reflects circularly polarized light in a specific wavelength range. Since the wavelength of reflected light determines its color, the perceived color

S0024-9297(97)01145-5 CCC: $15.00
Published on Web 08/06/1998

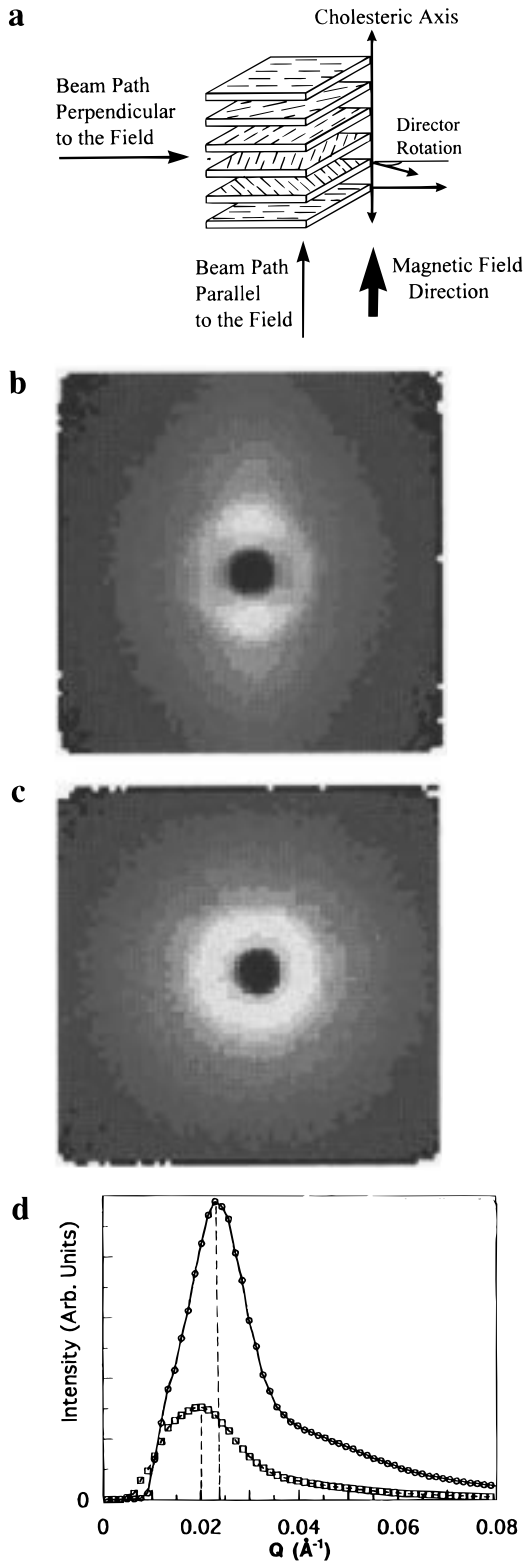

Figure 1. (a) Schematic model of the chiral nematic phase showing a "twisted" stacking of nematic planes. During SANS data collection from samples of dissolving pulp ($C = 7.7$ wt %) the neutron beam path was oriented (b) perpendicular and (c) parallel to the magnetic field direction. In the 2-D (I vs q) scattering patterns the colors correspond to intensity, where intensity increases from white to dark blue to magenta to red to yellow. The data confirm that the chiral nematic axis (or cholesteric axis) is parallel to the magnetic field and support the simple schematic picture in (a). In (d), the peak positions of the fitted I vs q curves are at different positions for the two orientations. This implies that rods are packed more closely in one direction.

of the film depends on the pitch of the cholesteric order and the angle of incidence of the light. The color of the reflected polarized light is "tunable", since the final pitch varies depending on processing variables such as the length of the microfibrils, the salt content, and the source of the cellulose microfibrils, all of which will be explored in this paper. One possible application of these cellulose films is as "high security" papers, inks, or films since their optical properties are not reproducible by simple printing or photocopying.

The agricultural community's interest in acid-hydrolyzed cellulose microfibrils is 2-fold. First, some of the microfibrils with the most interesting rheological and practical properties have been obtained from agricultural byproducts, such as cotton, sugar beet fiber, wheat straw, and bagasse. Second, there is evidence that introducing these cellulosic materials into starch composites results in "degradable polymers" with significantly higher modulus and better flexibility than starch alone.[8] In all of these applications, a full understanding of the rheology of these cellulosic suspensions is critical.

In the present study we use neutron scattering techniques to explore the nature of the liquid crystalline alignment of acid-hydrolyzed cellulose suspensions and its effect on rheology. As will be discussed, liquid crystalline interactions vary with magnetic field direction, microfibril concentration, salt levels, microfibril size, and shear flow conditions. During scattering experiments, an in situ shear cell was used in the neutron beam to investigate the effect of different shear conditions on microfibril alignment. Understanding the rheology will be critical for processing cellulose microfibrils in any application, especially considering that aqueous suspensions from cellulose microfibrils are highly shear sensitive fluids or gels, even at low concentrations.

Although X-ray scattering can be used to study cellulose microfibril suspensions,[1,9] neutron scattering has several advantages. By suspending samples in D_2O, a high neutron scattering contrast is achieved, allowing for collection of high-resolution data in a matter of minutes. Thus, samples do not change appreciably with sampling time. More importantly, neutrons are relatively nondestructive compared to X-rays. Samples can be monitored continuously for hours without concern for sample damage.

Experimental Section

Acid-hydrolyzed cellulose suspensions were formed from black spruce bleached Kraft pulp, dissolving pulp, or cotton fiber (from Whatman filter paper #4). Fibers were milled in a Wiley Mill to pass through a 40 mesh screen, added at 8% concentrations to ~60% sulfuric acid at 60 °C, and stirred for 30 min. To stop the reaction, distilled water at a 10:1 ratio was added, and the resulting suspension was centrifuged and washed repeatedly until the pH was above 1. The remaining acid and salt were removed by dialysis and ion exchange until the microfibrils were acid free. The chemically bound sulfur was determined by titration and standard elemental analysis and corresponded to a sulfation of about 10% of surface anhydroglucose units or roughly 0.2 sulfate groups/nm^2. The presence of surface charge allowed these suspensions to remain stable indefinitely. Above critical concentrations usually greater than ~1.5% (w/w), the suspensions separated into two phases, with the denser lower phase exhibiting birefringence indicative of the chiral nematic phase. Electron microscopy provided clear evidence that longer rods settled into the lower phase preferentially. Size fractionation was accomplished by repeated phase separation. Fraction one was the anisotropic

phase separated from the first biphasic suspension. Fraction two was obtained by concentration of the first isotropic phase until it formed a second phase, at which point the anisotropic phase was saved. Fraction three was obtained similarly. Although polydispersity has not been measured for these samples, it is presumably reasonably high (2−2.3) based on estimates from similar samples using electron microscopy and image analysis.

Neutron scattering data were collected at the NIST Center for Neutron Research, Gaithersburg, MD, using the NG3 small angle neutron scattering (SANS) beamline. "Cold" neutrons with a wavelength, λ, of 5 Å and full-width-at-half-maximum $\delta\lambda/\lambda$ of either 0.10 or 0.15 (depending on resolution requirements) were collimated using a 12.5 mm diameter aperture (except for the 2 × 12 mm vertical slit used for the shear cell when the beam path was parallel to the flow direction). Scattering intensity was measured using a 2-D area detector as a function of q, the magnitude of the scattering vector where $q = 4\pi \sin\theta/\lambda$ and 2θ is the scattering angle. The 2-D detector allowed for easy distinction of anisotropic scattering patterns. Intensity data were corrected for noncurvature and nonuniformities of the detector. Most samples were measured with the sample to detector distance and the source to sample distance roughly equal at 7 m. For several of the more dilute samples, a lower q configuration was used with distances of 13 m. Interference peaks were fit using nonlinear regression models by assuming Gaussian peak shapes with partial Lorentzian properties. Throughout this study, Bragg's law was assumed, in which the distance between planes of aligned rods, d, was related to q by $d = 2\pi/q$.

Cellulose microfibrils were freeze-dried and resuspended in D_2O using ultrasound at concentrations ranging from 0.5 to 13% (w/w). Magnetic alignment was achieved using a 2.0−2.4 T magnet. Once aligned, the samples were removed from the magnetic field and positioned in the neutron beam at different orientations relative to the chiral nematic axis (which corresponds to the magnetic field direction). Shear experiments were carried out in the neutron beam using a specially designed Couette shear cell[10] consisting of concentric quartz cylinders, which are nearly transparent to neutrons. Samples were sheared within the 0.5 mm gap between the two 65 ± 0.25 mm cylinders by rotating the outer cylinder at controlled rates while the inner cylinder (the stator) remained fixed. A schematic view of the shear cell geometry is presented in Figure 4a, highlighting the two distinct beam paths through the sample—parallel and perpendicular to the shear flow direction. Temperature within the sample annulus was controlled to 25 ± 1 °C using circulated heating fluid in contact with the stator. Rheological properties were also measured concomitantly on these samples outside of the beam using a Bohlin (VOR) rheometer with Couette geometry at 25 ± 0.5 °C. The order parameter, S, was calculated from SANS data by following a technique put forth by Oldenbourg et al.,[11] as described in the appendix.

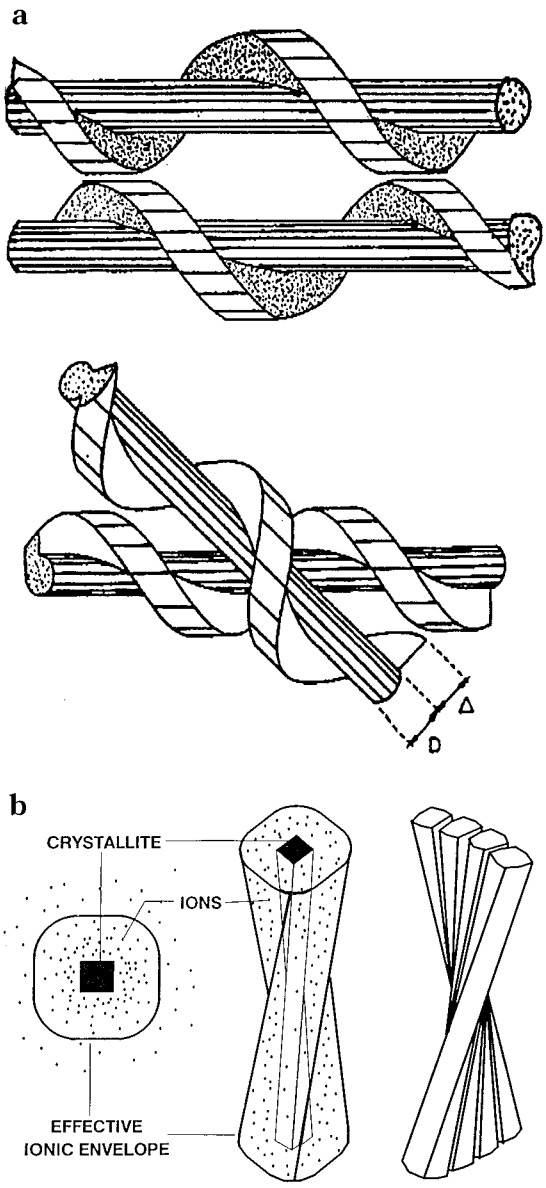

Figure 2. Representations of the tighter packing achievable by the chiral interaction of twisted rods. In (a), the distance between rods ($D + 2$) is reduced to $\sim D$ if, instead of rods packing with axes parallel, they pack with the "thread" of one rod fitting into the "groove" of its neighbor. For microfibrils with an electrostatic double layer (b), a threaded rod would alter the surrounding electric double layer and affect packing over relatively large distances.

Results and Discussion

Without a magnetic field or a shear field to enhance liquid crystalline ordering of cellulose microfibrils, the 2-D small angle neutron and X-ray scattering profiles are isotropic "powder" patterns.[1,9,12,13] The ring in the data is circularly averaged to give a scattering curve, I vs q, which is a single broad peak, corresponding to random alignment of microfibrils at a common average distance. Magnetic and shear alignment of the cellulose microfibrils results in anisotropic scattering patterns, which provide valuable insight into details of their liquid crystalline interactions.

Magnetic Field-Induced Orientation of the Liquid Crystalline Phase. 2-D scattering patterns represented as 2-D color contour plots were obtained from magnetically aligned cellulose microfibrils with the neutron beam path perpendicular (Figure 1b) and parallel (Figure 1c) to the magnetic field direction. Considering that the beam is 12.5 mm in diameter, it is clear that magnetic alignment creates a single uniform phase for relatively large samples. These data from dissolving pulp in D_2O (concentration, $C = 7.7\%$) provide clear evidence in support of the simple cholesteric model shown in Figure 1a. (In the figures the horizontal and vertical directions correspond to q in the x and y directions, respectively, and the colors correspond to intensity. Intensity increases from white to dark blue to magenta to red to orange-yellow.) The distinct reflections in the 2-D data when the beam is perpendicular to the field (Figure 1b) confirm that the microfibrils are aligned perpendicular to the magnetic field, in line with the idea that nematic planes are flat and in register. When the beam path is parallel to the magnetic field (Figure 1c), an isotropic "powder" pattern

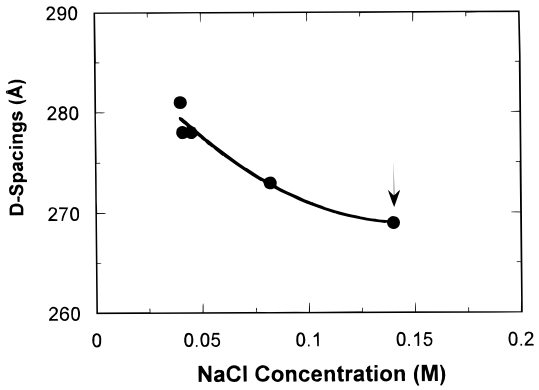

Figure 3. Effect of salt on *d* spacings of (●) cotton cellulose microfibrils at a concentration of 7% (w/w). The arrow marks the concentration at which the samples aggregate. (The line is included to guide the eye.)

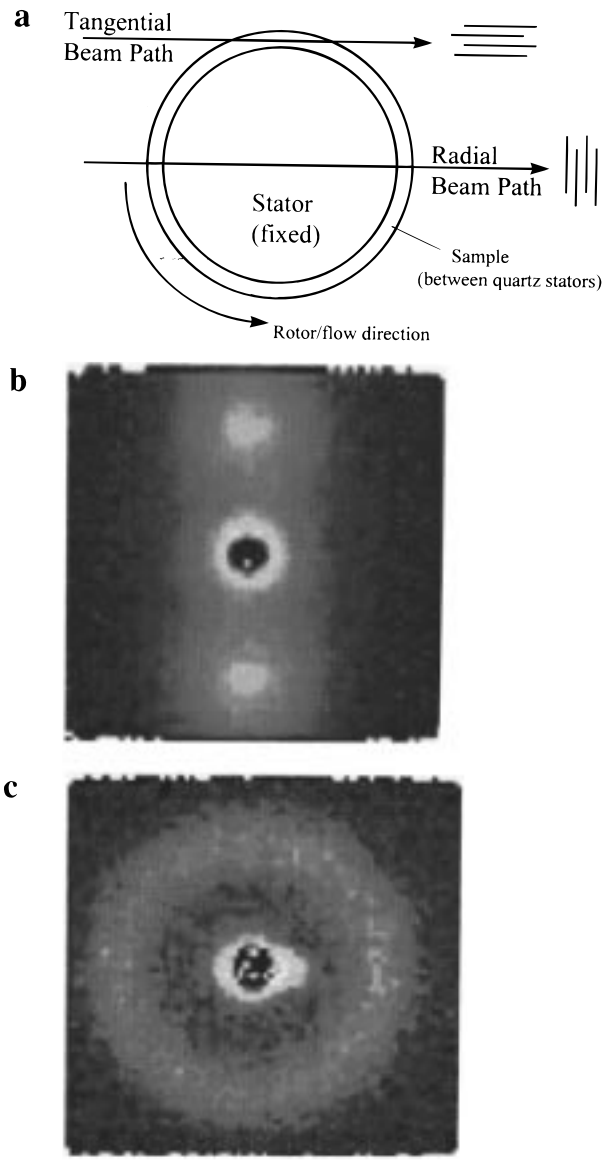

Figure 4. (a) Schematic top view of the Couette shear cell. SANS data were collected and represented as 2-D neutron scattering patterns (*I* vs *q*) with the beam path crossing through the cell either (b) in a radial path, and perpendicular to the flow direction, or (c) in a tangential path and parallel to the flow direction.

is observed. The interference peak here implies that the microfibrils within a nematic plane are at a common

Table 1. Comparison of the *d* Spacings Derived from Magnetically Aligned Cellulose Microfibrils in D_2O with the Beam Path Directed Perpendicular and Parallel to a ~2 T Magnetic Field Direction[a]

sample	*d* spacing (nm) with the beam perpendicular to the cholesteric axis	*d* spacing (nm) with the beam parallel to the cholesteric axis
1. dissolving pulp $C = 7.7\%$	28.1 ± 1.2	31.8 ± 0.8
2. cotton $c = 7.3\%$	35.6 ± 0.3	36.5 ± 0.3
3. cotton $C = 7.11\%$, 1 mM added NaCl	36.4 ± 0.8	38.0 ± 0.4
4. cotton[b] $C = 11.0\%$	28.0 ± 0.3	28.2 ± 0.3
5. cotton[b] $C = 13.1\%$	25.7 ± 0.3	26.3 ± 0.3
6. black spruce[b] $C = 2.7\%$	44.5 ± 0.4	45.1 ± 0.3
7. black spruce[b] $C = 3.2\%$	35.7 ± 0.4	36.1 ± 0.3
8. black spruce $C = 6.5\%$	27.4 ± 0.4	28.2 ± 0.3

[a] In the chiral nematic phase, this corresponds to a beam path alignment perpendicular and parallel to the cholesteric axis. For these samples, wavelength resolution (i.e., the full-width-at-half-maximum $\delta\lambda/\lambda$) was tightened to 0.10 Errors represent 95% (t-distribution) confidence levels using 3−5 replicate samples. [b] The *d* spacings calculated from the two beam orientations are not statistically different.

average distance. The scattering is isotropic because the microfibrils are arranged at multiple angles relative to the beam direction; i.e., the neutron beam passes through multiple nematic planes "seeing" rods aligned in many directions perpendicular to the cholesteric axis. These data confirm that the magnetic field is in the same direction as the cholesteric axis and are in keeping with optical and electron micrographs of the chiral nematic phase taken previously by Revol et al.[4,5]

The simple schematic representation of the chiral nematic phase outlined in Figure 1a is remarkably applicable for this system, although this is not the case for all systems. For the cholesteric arrangement of DNA molecules in water, scattering experiments have not produced such distinct anisotropic scattering patterns.[14,15] There are two possible explanations for this. One is that the relatively flexible DNA molecules have undulations along the DNA chains that create "ripples" in the nematic planes so that the nematic planes are not in register over relatively large distances. Another, simpler explanation, is that a much higher degree of orientation has been obtained in our experiments.

Source of the Chiral Interaction. In a previous paper[12] we presented preliminary data to describe the nature of the asymmetry inherent in the cellulose microfibrils. Although no chirality has been observed for these microfibrils, there must be some asymmetry in the particles to form a chiral nematic phase without any additional chiral agent. To explore this, the *d* spacings of the anisotropic peaks obtained with the neutron beam perpendicular to the magnetic field (as in Figure 1b) were compared with those parallel to the field (as in Figure 1c). Figure 1d is an example of such a comparison. For the isotropic patterns, scattering curves were derived from circular averaging of the intensity in all directions as a function of *q*, while for the anisotropic peaks, the 2-D pattern was sector averaged, in which only data at angles ±15° of the peak were used to create a scattering curve (*I* vs *q*). Peaks were fit using a linear least squares regression program, Bragg's law was invoked to obtain *d* spacings, and 3−5 replicate measurements were made for each sample (as outlined in Table 1). Curiously, for some of these samples, the *d* spacings between nematic planes are significantly less than between rods within a plane.

For sample 1, a difference greater than 12% is found, which is far from negligible, if we consider that the margin of error is only about 3% for this experiment. This difference can also be seen in Figure 1d. Sample 3 exhibits a smaller but still significant difference of about 5%. For several other samples examined the differences are less significant when compared to the experimental error, but there is nevertheless a detectable trend. The reason for these inconsistent results is not known but may well be due to the degree of orientation of the liquid crystalline phase. Indeed, although no degree of orientation ordering has been calculated for this series of experiments, samples 1 and 3 produced a 2-D pattern having a qualitatively higher anisotropy, an indication of a better orientation. By a simple observation of the arcing of the anisotropic peaks, it is clear that sample 1 exhibits the best orientation, followed by sample 3. The less distinct reflections of the other samples reveal that they are less oriented. If there is a difference between the parallel and perpendicular q values, any decrease of the degree of orientation will necessarily shift them toward some intermediate value. If the difference is small to start with, the disorientation can mask it entirely. We suspect that all samples would show the same significant differences as samples 1 and 3 if a sufficiently strong magnetic field could orient them to the same degree. Even better would be an experimental setup in which such a strong field could be maintained during the scattering, preventing relaxation of the samples. We have observed (data not shown) that relaxation after magnetic alignment depends on (i) concentration (lower concentration corresponds to faster relaxation), (ii) source of cellulose (liquid crystals from cotton relax faster than those from wood, likely due to differing fiber lengths), and (iii) ionic conditions (higher ionic strength corresponds to faster relaxation). Obviously, more work is necessary to confirm these findings.

The implication of a difference in d spacings observed in the two different orientations relative to the magnetic field is that the microfibrils pack tighter along the cholesteric axis than in the nematic planes perpendicular to it. This would support Straley's hypothesis that source of the chiral interaction[16] is directly attributable to packing of screwlike rods. As shown in Figure 2, threaded rods can be packed more tightly when their main axes are offset such that their "threads fit within the each others' "grooves".[16] Even a small twist in the cellulose microfibril would be sufficient to induce the observed chiral interaction. It is difficult to conceive of a mechanism other than that which was previously proposed[6] that would work at the reasonably long-range interparticle distances seen here. A recent microscopic study of algal cellulose using TEM and AFM supports the presence of such a chiral twist along the microfibrils.[17]

Effect of Ionic Strength. Another issue for polyelectrolytic polymers worth exploring here is the idea that, in the anisotropic phase of a biphasic system, the average interparticle distance decreases with the addition of salt. Application of simple double layer principles implies that counterions in solution shield the surface charges and reduce the effect of Coulombic repulsion. The data in Figure 3 show that this effect seems to be relatively insignificant for charged cellulose microfibrils up to the point at which they "salt out". Similar to results reported previously,[9] there is little if any decrease in microfibril spacing with increasing salt. Then, at NaCl concentrations above ~0.15 M, the system aggregates and the interference peaks disappear. This result is not surprising for such a system, since in a previous report[18] it has been shown that the addition of salt to a biphasic system did not significantly change the concentration of particles in each phase, although it greatly changed the relative proportions of each phase.

The behavior seen here is qualitatively similar to that seen by Wang and Bloomfield[14] for DNA suspensions, but contrary to trends seen for suspensions of tobacco mosaic virus (TMV).[19,20] TMV d spacings show a relatively steep drop off of d spacing with added salt over this same concentration range. Such a difference in behavior from TMV is necessarily expected since both acid-hydrolyzed cellulose microfibrils and TMV are ionic rodlike particles. One obvious difference is that the cellulose suspensions are not monodisperse, contrary to the TMV system.

Shear-Induced Alignment of Cellulose Microfibrils. With increasing concentration, cellulose microfibril suspensions become increasingly gellike and exhibit higher viscosities. It is difficult to imagine processing such gels without altering the structure by shear. Observations with polarized filters reveal that the "fingerprint" patterns indicative of the chiral nematic phase are deformed and disappear with increasing shear rate. Data obtained here from an in situ shear cell placed in the neutron beam provide evidence that, as shear disrupts the chiral nematic phase, microfibrils exhibit nematic ordering with the microfibrils aligned parallel to the flow direction. SANS patterns were measured with the beam passing through two different paths of the shear cell, as outlined schematically in Figure 4a. When the beam path is through the center of the concentric cylinders of the shear cell, and is thus perpendicular to flow direction, the scattering pattern exhibits distinct anisotropic interference peaks, as shown in Figure 4b for black spruce microfibrils (C = 7.7% w/w) sheared at 7000 s^{-1}. These interference peaks correspond to alignment of rods parallel to the flow direction and are at a momentum transfer, q, of 0.282 nm^{-1} (derived from sector averaging of intensity at angles ±15° around the peak maximum). The scattering pattern from the same sample under the same conditions using the tangential beam path geometry is an isotropic ring pattern, as shown in Figure 4c. The maximum of this isotropic peak occurs at the same q as the anisotropic peaks. For the tangential beam path, the beam and the flow direction are in the same direction; thus, the microfibrils are most likely aligned parallel to the beam and arranged with a common average spacing.

Shear-Induced Packing of Cellulose Microfibrils. It would be of great interest to determine the type of microfibril packing induced by shear alignment. There have been several reports of shear-aligned polymer suspensions in which the hexagonal order is in register over large enough sample areas to produce distinct anisotropic scattering patterns.[21,22] However, the scattering from a shear-aligned cellulose suspension shown in Figure 4c is an isotropic powder pattern with no anisotropic behavior. This does not rule out locally ordered packing, but more likely implies that different ordered regions, if present, are not in register over a large area relative to the beam size.

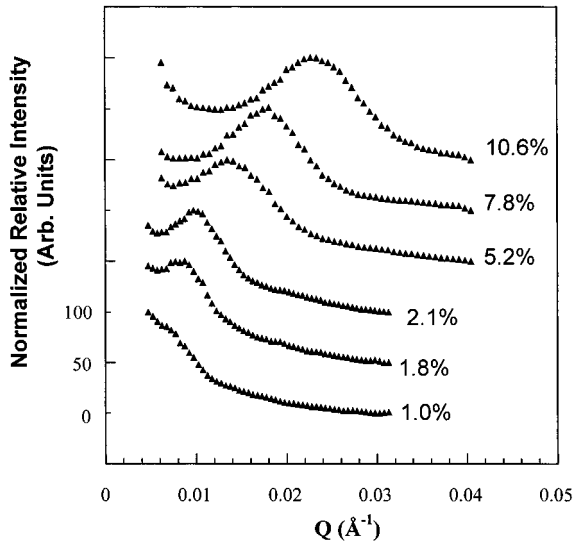

Figure 5. Neutron scattering curves (I vs q) of black spruce cellulose microfibrils at different concentrations, noted to the right of each curve. For clarity, intensities have been normalized and offset by 50 units with respect to each other in a series. At higher concentrations microfibrils pack tighter, and the peak in the data moves to higher q. The peak positions determined from fitting these data were used as a basis for Figure 6.

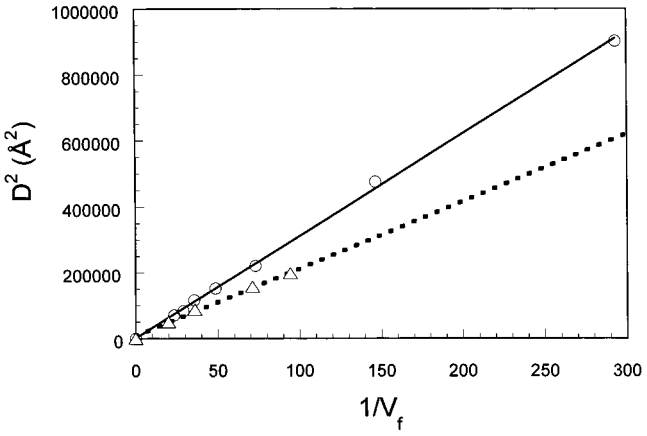

Figure 6. Plot of d^2 vs $1/V_f$. Cellulose was derived from black spruce suspensions in the (●) first and (▲) third fractionations with lengths of approximately 280 and 180 nm, respectively.

Size Evaluation. The scattering patterns of these colloidal suspensions under shear are obviously dependent on sample concentration,[12,13] as shown in Figure 5. As the concentration is increased, the position of the interference peak moves to a higher q value, which implies tighter packing of microfibrils. Similar general trends with concentration are also seen for randomly aligned and magnetically aligned microfibril samples. The relationship between concentration and q was used to determine the lateral size of the colloidal particles—information which had been estimated in previous reports using laborious electron microscopy imaging techniques.[4] Considering Bragg's law, where $d = 2\pi \sin \theta/\lambda = 2\pi/q$, it can readily be shown[14] that an array of long randomly packed microfibrils (i.e., rods with $L/a > 20$) will have d spacings, $d = (a^2/V_f)^{1/2}$, where L and a are the length and width of the microfibril, respectively, and V_f is the volume fraction. Based on this relationship, data were plotted in Figure 6 in the form d^2 as a function $1/V_f$. From the slopes of these linear plots, the microfibril width, a, was calculated. Two samples were used, the first and the third fractions of the cellulose suspension from wood pulp, obtained as described in the Experimental Section, and having average lengths of approximately 280 and 180 nm, respectively. The values of the calculated widths were $a = 5.6$ nm for the first fraction and $a = 5.15$ nm for the third fraction. Both calculated values are reasonable dimensions for cellulose microfibrils from wood, although they are slightly higher than the dimensions measured by transmission electron microscopy (TEM).[4] Typical values for individual crystallites observed by TEM are 5.0 nm.

The calculation of the above values was made by using random lateral packing. If the packing is assumed to be a local hexagonal packing, the formula $d_{hex} = (a^2 \cos 30°/V_f)^{1/2}$ applies and the values will be $a = 6.0$ nm for the first fraction and $a = 5.5$ nm for the third. The values calculated here assuming either hexagonal or random lateral order are higher than the TEM values measured previously. There is a high likelihood of aggregation in the cellulose suspensions, which would lead to inaccuracies in estimates of the average lateral dimensions. Such aggregates, usually doublets or triplets, are indeed observed in TEM preparations but were not included in the size determination by image analysis.

Particle Size Effects on Shear-Induced Orientation. Variations in the microfibril dimensions are key parameters in determining both the relative order obtained by these suspensions under shear and their relaxation behavior after shear is terminated. Both the first and third fractions, with lengths of ~280 and 180 nm, respectively, develop significant shear-induced order. Figure 7 is a series of 2-D color contour plots for the two fractions of the SANS intensity data as a function of q. Note that the radial beam path is used, in which the beam path is perpendicular to the shear flow direction. The flow direction is thus from left to right in each of these surface plots. As the shear rate is increased from 0.1 to 7000 s^{-1}, the SANS peaks at q perpendicular to the flow direction become more distinct, corresponding to increased alignment of microfibrils with increasing shear.

From the 2-D data the order parameter, S, was calculated as described in the Appendix. Basically, relative peak sharpening was used to quantify the shear-induced ordering of the two fractions of cellulose microfibrils. Figure 8 shows that S increases most rapidly at shear rates between 0.2 and ~100 s^{-1}, and reaches a plateau above 100 s^{-1}. Although both the first and third fractions result in a similar ordering behavior, the first fraction (with $L = 280$ nm and at a concentration, C, of 5% w/w) reaches a higher degree of order than the third fraction (with $L = 180$ nm and $C = 7\%$ w/w). A higher concentration was used for the third fraction so that the viscosities of the two samples would be equivalent.

Apparently, the key parameter in the higher order obtained from the first fraction is the axial ratio, L/a. The first fraction has an axial ratio of ~47, while that of the third fraction is ~33. It should be noted that the samples were already anisotropically aligned before starting the experiment because some order was introduced while injecting the sample into the Couette shear cell. Shear history is difficult to "erase" for some of these samples, since it may take days to relax to random order.

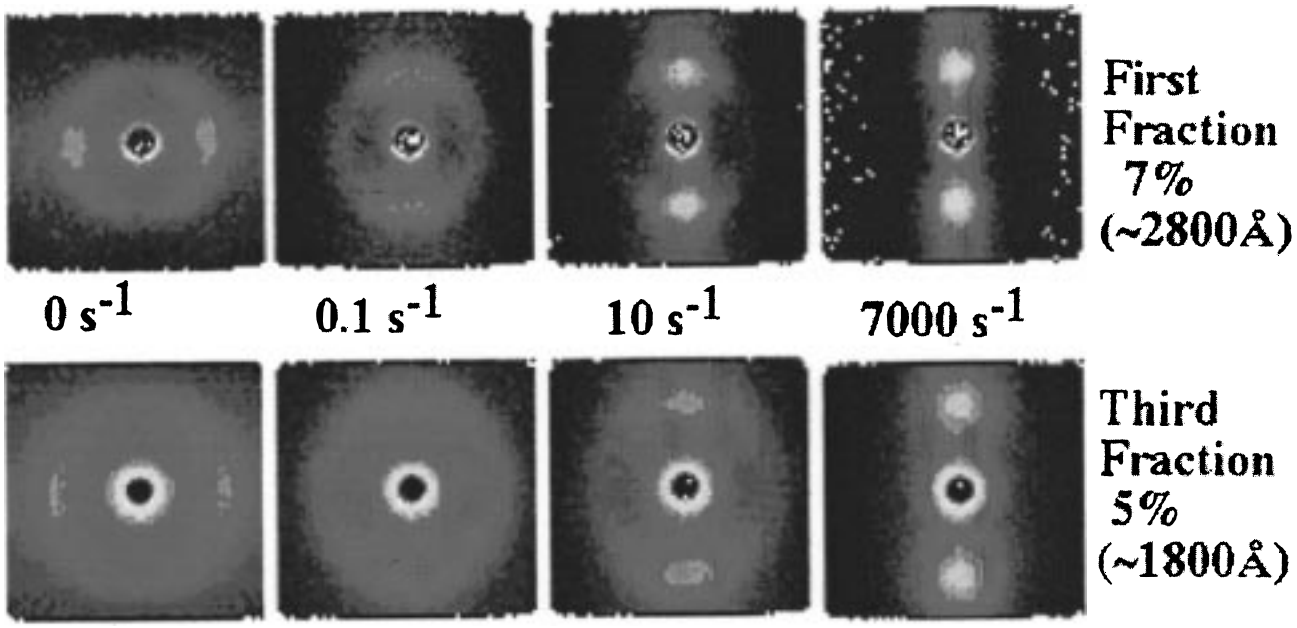

Figure 7. Series of 2-D color contour plots showing the shear-induced alignment of first (top row) and third (bottom row) fractions of black spruce microfibrils. The corresponding shear flow direction is from left to right in these scattering patterns.

To correlate "bulk" behavior with structural information, a fraction of each sample was used to obtain the viscosity/shear profile on an independent viscometer. The viscosity vs shear rate profile for the first fraction of microfibrils is plotted in the same figure as the order parameter data (Figure 8). This profile shows model behavior for liquid crystalline polymers, in keeping with a theoretical description put forth by Onogi and Asada.[23] At very low shear rates there is a shear thinning region where tactoids, i.e., chiral nematic domains, begin to flow against each other (regime I). At intermediate shear rates there is a plateau in the viscosity vs shear rate profile where domains start to break up (regime II). At higher shear rates there is a further shear thinning region where individual rods are free to align further (regime III). This behavior has been demonstrated in detail for charged rods of chitin crystallites that are similar in dimensions but of opposite charge to cellulose.[24]

It is interesting to correlate the two measurement techniques—viscosity, which reflects a bulk property of the system, and SANS, which measures order on the macromolecular/interparticle scale (see Figure 8). The SANS order parameter shows that the most rapid alignment of rods occurs at roughly the same shear regime as the plateau in the viscosity profile, where domains are hypothesized to be breaking up.[23] In the so-called shear thinning regime at the highest shear rates both curves reach a plateau at roughly the same values. This result is similar to X-ray measurements by Picken et al.[25] of the order parameter for polyaramid solutions in which there was no further ordering in the shear thinning region for shear rates above 1000 s^{-1}.

Relaxation after Shear-Induced Alignment. Although there is a significant difference in the ordering behavior of the two fractions of microfibrils, there is a greater difference in their relaxation behavior after shear ceases. In Figure 9 relaxation behavior is shown for the first and third fractions in the form of 2-D contour plots. These data are then used to derive Figure 10, a plot of the order parameter vs the time after the shear has ceased. Relaxation from shear-induced alignment for the third fraction (i.e., the shorter microfibrils) is characterized by a loss of anisotropic structure in the contour plots and a rapid decrease in the order parameter. Relaxation to isotropic scattering is complete within 1 h. In contrast, *S* for the first fraction with longer microfibrils decreases at a much slower rate, with anisotropic scattering remaining for many hours. Interestingly, after 5 min of shear relaxation in the first fraction, the shear-induced order does not decrease at all. The calculated order parameters are 0.89 ± 0.02 during shear at 7000 s^{-1} and 0.92 ± 0.02 after shear cessation.

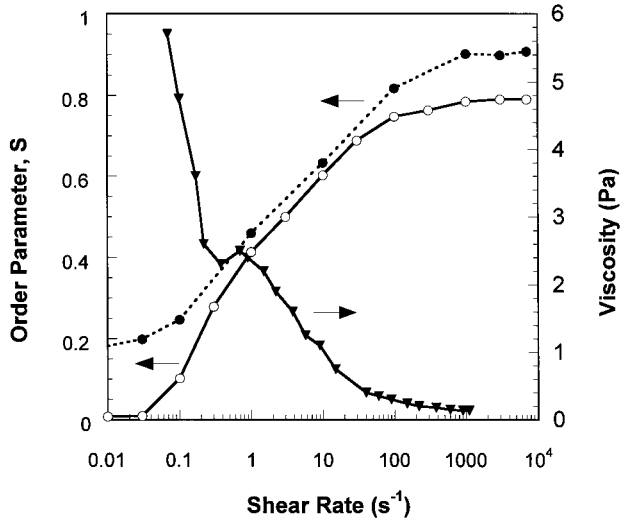

Figure 8. Effect of shear rate on the order parameter, *S*, for the (●) first and (○) third fractions. Also plotted here is (▼) the viscosity profile (in Pa) of the first fraction as a function of shear rate. There are correlations between the two very different techniques.

Complex relaxation behavior such as increased molecular orientation after shear ceases has been observed previously by Hongladarom et al.[26] in liquid crystalline solutions of poly(benzyl glutamate). They used polarized light to measure flow birefringence and saw nonlinear "ringing" in their relaxation curves and indica-

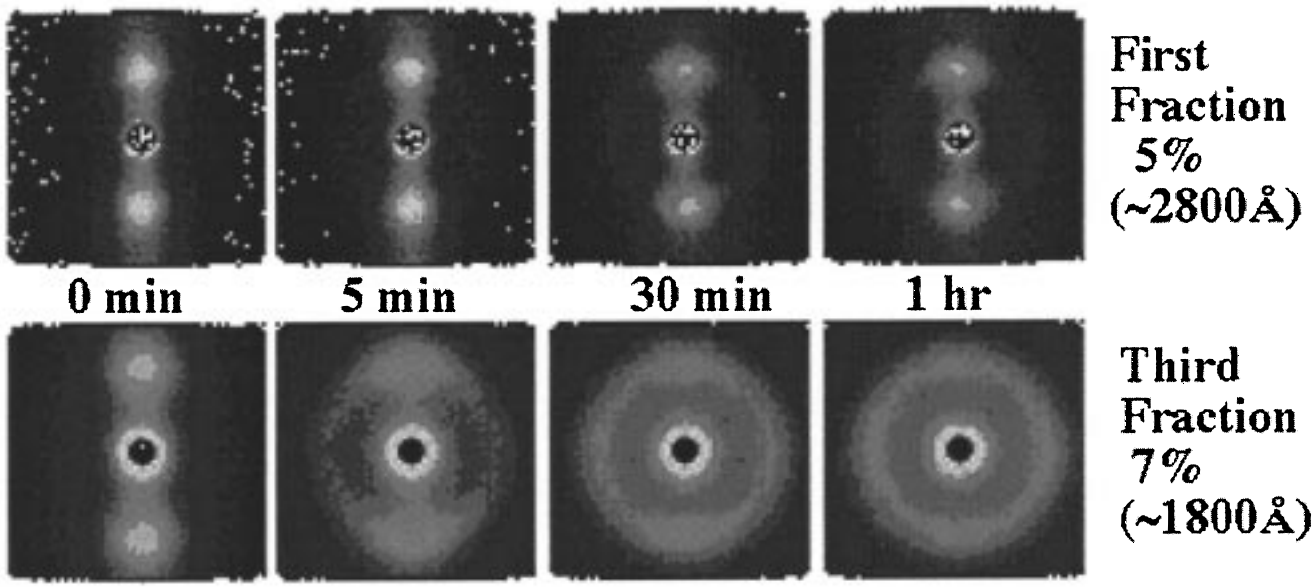

Figure 9. Relaxation behavior of cellulose microfibril suspensions after shear at 7000 s^{-1} represented by 2-D color contour plots taken at different time intervals. The two fractions from the same sample vary in size. The third fraction, with $L/a = 33$ and at a concentration of 7% (w/w), relaxes far more rapidly than the first fraction, with $L/a = 47$ and at a concentration of 5% (w/w).

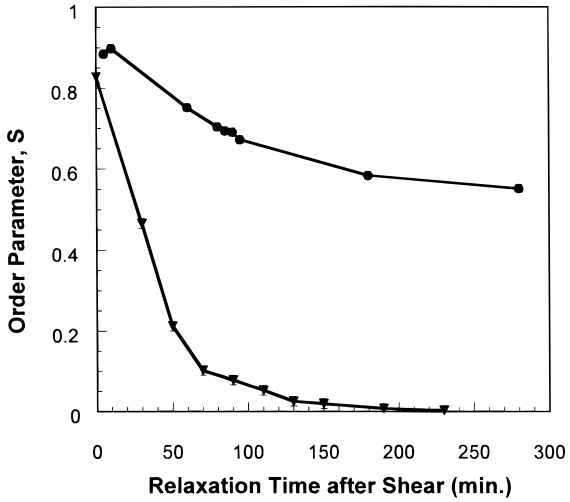

Figure 10. Relaxation behavior of cellulose microfibril suspensions after shear at 7000 s^{-1} represented by a plot of the order parameter as a function of time after shear. The third fraction (▼), at 7% concentration and with $L/a = 33$, relaxes far more rapidly than the first fraction (●), at 5% concentration, with $L/a = 47$.

tions of an increase in the average molecular orientation well after shear ceased. One possible explanation for the increasing order after shear ceases is to consider the uneven forces on a rod within a shear field. In a Couette shear cell such as used here, the velocity profile is not flat across the sample gap. This creates constant torque on the rods during shearing, which would induce rod "wobbling". Wobbling rods would have the tendency to tumble easily in the flow if not for their interaction with neighboring microfibrils. When the shear field subsides, the wobble subsides, and the rods exhibit higher order, at least at the early stages of relaxation. This behavior would depend on viscosity and microfibril length.

Particle undulations or "wobbling" have played a significant role in describing the ordering of DNA.[27,28] The undulation of long polyelectrolytic rods increases the effective diameter of the charge field around each particle such that intermolecular forces are enhanced by an order of magnitude relative to perfectly rigid rods.[29] The shear cell scattering studies such as presented here may present an interesting way to vary the degree of wobbling for rodlike particles, and thus be used to gain a better understanding of the role of undulations on polyelectrolyte polymer systems.

Conclusions

Aqueous suspensions of acid-hydrolyzed cellulose microfibrils are an ideal model system to study the liquid crystalline interactions of rodlike ionic species. Samples can be obtained that vary in length, width, charge density, and size polydispersity. We have performed in situ SANS measurements of the magnetic and shear alignment of polyelectrolytic, liquid crystalline cellulose microfibrils in aqueous suspension. *d* spacing measurements suggest that microfibrils pack tighter along the cholesteric axis than perpendicular to it. This lends support to the hypothesis that cellulose microfibrils are twisted rods, perhaps due to strain in their crystalline microstructure.[6] Although such an asymmetry has only recently been mentioned, it is difficult to imagine other scenarios to explain the observed *d* spacings and a chiral interaction at such a long range in the absence of additional chiral agents.

The anisotropic SANS scattering patterns observed during shear alignment exhibit interparticle interference peaks perpendicular to the shear flow direction. These peaks sharpen with increasing shear rate, with observed order parameters up to 0.9 for shear rates >1000 s^{-1}. Apparently, the chiral nematic ordering is disrupted in favor of a nematic ordering in which rods align with their long axis in the direction of fluid flow. The axial ratio is a key parameter in determining the degree of shear-induced order, as well as the relaxation behavior after shear ceases. The viscous suspensions derived from long microfibrils (~280 nm) remain aligned for hours and even days after shearing, while samples with shorter microfibrils (~180 nm) relax quickly. The relationships between macromolecular structure and bulk rheology explored here are critical in developing

processing conditions for these novel cellulosic microfibril fragments.

Acknowledgment. We thank Boualem Hammouda, John Barker, and Mark Dadmun, for many helpful discussions and technical advice, as well as Adrian Parsegian and his colleagues for several useful suggestions. SANS measurements were performed on the NIST-NSF NG3 30 m instrument, which is supported by the National Science Foundation (NSF) under agreement No. DMR-9122444. W.J.O. would like to acknowledge NSF for financial support during his tenure at NIST. R.H.M thanks the Natural Sciences and Engineering Research Council (NSERC) and Xerox Corp. for ongoing support.

Appendix

The order parameter, S, was calculated from SANS data by following a technique put forth by Oldenbourg et al.[11] Relative ordering of the samples was correlated to peak sharpening by measuring the relative width of azimuthal peak traces, i.e., the width of a peak along an arc at a fixed radial distance from the center of the pattern. Basically, the azimuthal peak width intensity $G(\Phi)$ along an arc defined by the angle Φ from the equator can be related to the orientational probability distribution, $f(\beta)$, of finding a rod tilted at an angle β with respect to the director. The azimuthal peak width is then

$$G(\Phi) = \int I_s(\omega)\, f(\beta) \sin \omega \, d\omega \qquad (1)$$

where $I_s(\omega)$ is the single rod intensity function of a rod tilted at an angle ω with respect to the incoming beam direction. Several assumptions were made to simplify this expression. First, $f(\beta)$ was assumed Gaussian with a peak width of α, which is assumed very small (i.e., the angular spread of the rod axis around the director is small). Second, by noting that the neutron beam direction is perpendicular to the director (or shear flow direction), the relationship between angles Φ, ω, and β is simply $\beta = \cos^{-1}(\cos \Phi \sin \omega)$. With these simplifications $G(\Phi)$ becomes

$$G(\Phi) = A \exp\left(-\sin^2 \frac{\Phi}{2\alpha^2}\right)\left[\frac{1}{\cos \Phi} + \frac{\alpha^2}{2 \cos^3 \Phi} + ...\right] \qquad (2)$$

where A and α are adjustable fitting parameters. The parameters A and α are used to define the Gaussian orientational distribution $f(\beta)$, which is then used to calculate the order parameter S by

$$S = f(\beta)\, \frac{1}{2}(3 \cos^2 \beta - 1)\, d\beta \qquad (3)$$

References and Notes

(1) Marchessault, R. H.; Morehead, F. F.; Walter, N. M. *Nature* **1959**, *184*, 632.
(2) Immergut, E. H.; Ranby, B. G. *Ind. Eng. Chem.* **1956**, *48*, 1183.
(3) Mukkerjee, S. M.; Woods, H. J. *Biochim. Biophys. Acta* **1953**, *10*, 499.
(4) Revol, J.-F.; Bradford, H.; Giasson, J.; Marchessault, R. H.; Gray, D. G. *Int. J. Biol. Macromol.* **1992**, *14*, 170.
(5) Revol, J.-F.; Godbout, L.; Dong, X.-M.; Gray, D. G.; Chanzy, H.; Maret, G. *Liq. Cryst.* **1994**, *16* (1), 127.
(6) Revol, J.-F.; Marchessault, R. H. *Int. J. Biol. Macromol.* **1994**, *15*, 329.
(7) Revol, J.-F.; Godbout, D. L.; Gray, D. G. International Patent Publication No. WO 95/21901. 1995.
(8) Cavaille, J.-Y.; Dufresne, A. *Abstracts of the 5th Chemical Conference of North America*, November 11−15, 1997, Cancun, Mexico; 1997.
(9) Furuta, T.; Yamahara, E.; Konishi, T.; Ise, N. *Macromolecules* **1996**, *29*, 8994.
(10) Straty, G. C. *J. Res. Natl. Inst. Stand. Technol.* **1989**, *94*, 259.
(11) Oldenbourg, R.; Wen, X.; Meyer, R. B.; Caspar, D. L. D. *Phys. Rev. Lett.* **1988**, *61*, 1851.
(12) Revol, J.-F.; Orts, W. J.; Godbout, L.; Marchessault, R. H. *Polym. Mater. Sci. Eng.* **1994**, *71*, 334.
(13) Orts, W. J.; Godbout, L.; Marchessault, R. H.; Revol, J.-F. in *Flow-Induced Structure in Polymers*; Nakatani, A. I., Dadmun, M. D., Eds.; ACS Symposium Series, Vol. 597; American Chemical Society: Washington, DC, 1995; p 335.
(14) Wang, L.; Bloomfield, V. A. *Macromolecules* **1991**, *24*, 5791.
(15) Groot, L. C. A.; Kuil, M. E.; Van der Maarel, J. R. C.; Heenan, R. K.; King, S. M.; Jannink, G. *Liq. Cryst.* **1994**, *17*, 263.
(16) Straley, J. P. *Phys. Rev. A* **1976**, *14*, 1835.
(17) Hanley, S. J.; Revol, J.-F.; Godbout, L.; Gray, D. G. *Cellulose*, in press.
(18) Dong, X. M.; Kimura, T.; Revol, J.-F.; Gray, D. G. *Langmuir* **1996**, *12*, 2076.
(19) Parsegian, V. A.; Brenner, S. L. *Nature* **1976**, *259*, 632.
(20) Bernal, J. D.; Fankuchen, I. *J. Gen. Physiol.* **1941**, *25*, 111.
(21) Hamilton, W. A.; Butler, P. D.; Baker, S. M.; Smith, G. S.; Hayter, J. B.; Magid, L. J.; Pynn, R. *Phys. Rev. Lett.* **1994**, *72*, 2219.
(22) Bates, F. S. NIST Reactor: Summary of Activities, October 1993 through September 1994. NIST Technical Report; NIST: Washington, DC, 1994.
(23) Onogi, S.; Asada, T. In *Rheology*; Astarita, G., Marrucci, G., Nicolais, L., Eds.; Plenum: New York, 1980; Vol. 3.
(24) Li J.; Revol, J.-F.; Marchessault, R. H. *J. Colloid Interface Sci.* **1996**, *183*, 365.
(25) Picken, S. J.; Aerts, J.; Doppert, H. L.; Reuvers, A. J.; Morthholt, M. G. *Macromolecules* **1991**, *24*, 1366.
(26) (a) Hongladarom, K.; Burghardt, W. R.; Baek, S. G.; Cementwala, S.; Magda, J. J. *Macromolecules* **1993**, *26*, 772. (b) Hongladarom, K.; Burghardt, W. R.; Baek, S. G.; Cementwala, S.; Magda, J. J. *Macromolecules* **1993**, *26*, 785.
(27) Podgornik, R.; Rau, D. C.; Parsegian, V. A. *Macromolecules* **1989**, *22*, 1780.
(28) Evans, E. A.; Parsegian, V. A. *Proc. Natl. Acad. Sci. U.S.A.* **1986**, *83*, 7132.
(29) Odijk, T. *Biophys. Chem.* **1993**, *46*, 69.

MA9711452